Optimization of Heat Treatment Profiles Applied to Nanometric-Scale Nb_3Sn Wires With Cu-Sn Artificial Pinning Centers

D. Rodrigues, Jr., L. B. S. Da Silva, C. A. Rodrigues, N. F. Oliveira, Jr., and C. Bormio-Nunes

***Abstract*—Nb_3Sn is one of the most used superconducting materials for applications in high magnetic fields. The improvement of the critical current densities (J_c) is important, and must be analyzed together with the optimization of the flux pinning acting in the material. For Nb_3Sn, it is known that the grain boundaries are the most effective pinning centers. However, the introduction of artificial pinning centers (APCs) with different superconducting properties has been proved to be beneficial for J_c. As these APCs are normally in the nanometric-scale, the conventional heat treatment profiles used for Nb_3Sn wires cannot be directly applied, leading to excessive grain growth and/or increase of the APCs cross sections. In this work, the heat treatment profiles for Nb_3Sn superconductor wires with Cu(Sn) artificial pinning centers in nanometric-scale were analyzed in an attempt to improve J_c. It is described a methodology to optimize the heat treatment profiles in respect to diffusion, reaction and formation of the superconducting phases. Microstructural, transport and magnetic characterization were performed in an attempt to find the pinning mechanisms acting in the samples. It was concluded that the maximum current densities were found when normal phases (due to the introduction of the APCs) are acting as main pinning centers in the global behavior of the Nb_3Sn superconducting wire.**

***Index Terms*—Artificial pinning centers, heat treatment profiles, microstructural and superconducting characterization, Nb_3Sn.**

I. Introduction

TRANSPORT of high critical current densities (J_c) in high magnetic fields is important in some applications of superconductivity, like magnets for high energy physics (the Large Hadron Collider—LHC), nuclear fusion tests (the International Thermonuclear Experimental Reactor—ITER), and magnetic resonance [1], [2].

The optimization of the magnetic flux pinning in superconductors is one of the most important ways to improve the critical currents. The introduction in the superconducting matrix of normal phases, or a phase with distinct superconducting properties, is one very effective way to improve pinning because it adds new pinning centers to the microstructure already existent in the superconductor, mixing pinning types and mechanisms. This behavior is obtained by the introduction of Artificial Pinning Centers (APCs) [3].

Manuscript received August 03, 2010; accepted September 27, 2010. Date of publication December 23, 2010; date of current version May 27, 2011. This work was supported by FAPESP, CNPq, and CAPES, Brazil. DRJ, CBN, and NFOJ are CNPq researchers.

The authors are with the Departamento de Engenharia de Materiais, Escola de Engenharia de Lorena, Universidade de São Paulo, Lorena SP 12600-970, Brazil (e-mail: durval@demar.eel.usp.br).

Digital Object Identifier 10.1109/TASC.2010.2093104

Cu(Sn) APCs were recently introduced into Nb filaments using successive steps of mechanical deformation, following the solid-liquid method creating a new Nb_3Sn composite with nanometric-scale pinning centers [3]. The samples showed significant enhancement in their transport properties for a wide range of magnetic fields, compared to micrometric-scale conventional superconductors produced by the same approach [4]. The superconducting properties of this special material could be further improved by the optimization of the heat treatment (HT) profiles [5].

The HT profile used for Nb_3Sn superconducting wires is important to determine the transport properties of the final material. For conventional Nb_3Sn superconducting wires several studies were performed to optimize the HT profiles and improve the critical current densities (J_c), upper critical magnetic field and pinning force [6], [7].

Optimization of the heat treatment profiles for the nanometric-scale-APC Nb_3Sn superconducting wires is important and must be carefully designed due to the small dimensions of the APCs and the Nb filaments. The average grain size must be kept small, while the HT temperatures and times must still enable the diffusion, reaction and formation of the superconducting phases in the matrix, also maintaining the APC distribution. This is a complex task because the choice of the HT profiles must consider the small dimensions, and also the small Sn diffusion paths, existing in the system. The complete transformation of the Nb filaments into Nb_3Sn is obtained in reduced temperatures and times compared to conventional Nb_3Sn wires [3], [4].

In the present work, different HT profiles for Nb_3Sn superconducting wires with nanometric-scale Cu(Sn) APCs, were analyzed in an attempt to optimize the superconducting properties, improving the pinning forces and, consequently, the critical current densities. The influence on the upper critical magnetic field was also analyzed. Microstructural characterization and transport measurements were performed to verify the pinning mechanisms acting in the material.

II. Experimental Procedures

Solid-liquid diffusion method was used to prepare the samples, elsewhere described in [3]. The wire was deformed down to 1.06 mm in diameter, containing 1,064,514 Nb filaments with average diameter of 410 nm, 36 cores of Sn, and internal stabilization of Cu surrounded by a Ta diffusion barrier. The APCs have an average diameter of 40 nm.

TABLE I
HEAT TREATMENT PROFILES FOR THE APC Nb_3Sn WIRE

Sample	Temperature/time
1	575°C/200h
2	650°C/200h
3	700°C/100h
4	220ºC/100h+650°C/50h
5	480ºC/50h+650ºC/50h
6	575°C/50h+650ºC/50h
7	220ºC/100h+480ºC/50h+650ºC/100h

Sections of the wire were removed for HT optimization. Cu was electroplated on both ends of the samples to avoid leak of Sn during the HT at temperatures above the Sn melting point. After that, the samples were encapsulated in quartz tubes under an argon atmosphere of 20 mTorr. The HT already started with the required initial temperature and finished with quenching to room temperature. The HT profiles were used following the steps showed in Table I. After HT, samples were removed for microstructural characterization using a JSM 6330F Field Emission Gun Scanning Electron Microscope (FEG-SEM). These samples were polished and chemically revealed with nitric acid.

Superconducting characterization of the samples was performed in order to determine the quality of the superconducting phases, the critical temperatures T_c, and critical current densities J_c, consequently determining the influence of the introduction of the APCs and of the HT on the superconducting phases and on the global behavior of the samples, including magnetic flux pinning mechanisms analysis. Transport critical temperature $T_{cTransp}$ measurements were performed by the four probe method with an excitation current of 500 mA [8].

Transport measurements were performed by the four probe method using a 17 T (Cryogenic Inc.). The electric field criteria of 10 $\mu V/m$ was used to determine the critical currents [9]. All measurements were performed at 4.2 K (liquid helium bath) and under magnetic fields applied perpendicularly to the axis of the wire. It was supposed that during the transport measurements the electrical field was always sufficiently large to enable the conduction of supercurrents through the APCs, what contributes to the global pinning behavior together with the grain boundaries already present in the superconducting phase. In this way, the transport measurements should present the global pinning behavior of the superconducting wire.

III. RESULTS AND DISCUSSION

A. Microstructural Characterization

Fig. 1 compares the microstructures of the Nb filaments formed before and after HT using a single step at 575°C/200 h (sample 1), 650°C/200 h (sample 2), and 700°C/100 h (sample 3). The voids observed in the microstructures are the initial Cu(Sn) region etched with nitric acid during sample preparation. Fig. 1(a) shows the 127 monofilaments from the first bundling without heat treatment. For samples after HT (Figs. 1(b), 1(c), and 1(d)) the coalescence of the Nb filaments can be observed, changing the region to only one large filament with average diameter of 4 μm and with internal APCs of Cu(Sn) in the Nb_3Sn superconducting matrix. For high temperature of HT, the APCs decreased in number, whereas the average cross sections increased due to the increase of Sn diffusion into the Nb filaments at higher temperatures.

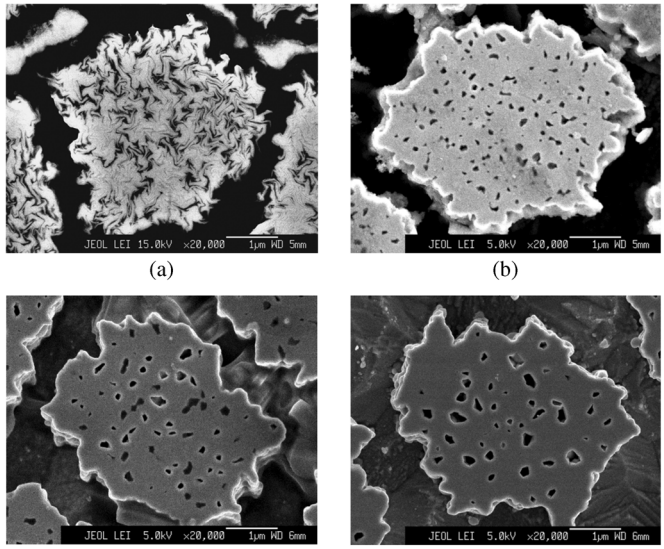

Fig. 1. Microstructures of the Nb filaments before HT (a) and after HT using: (b) 575°C/200 h (sample 1), (c) 650°C/200 h (sample 2), and (d) 700°C/100 h (sample 3). The micrographs were obtained in a FEG-SEM using secondary electrons.

TABLE II
CRITICAL TEMPERATURES BY TRANSPORT ($T_{cTransp}$)

Sample	$T_{cTransp.}$ (K)	ΔT_c (K)
1	16.6	0.4
2	17.3	0.5
3	16.4	0.3
4	17.1	0.3
5	17.3	0.2
6	16.6	0.3
7	16.5	0.5

B. Superconducting Characterization

Table II shows the critical temperatures extracted from the transport measurements, showing that all samples had almost the same critical temperature next to 17 K. The values of $T_{cTransp}$ from the transport measurements were determined as the mid-point of the resistive transition from the normal state to the superconducting state. The values of ΔT_c were defined as the width of the superconducting to normal transition and represent the quality of the Nb_3Sn superconducting phase formed after HT. The values of ΔT_c are around 0.4 K, meaning good quality of the superconducting phases formed after all HT. Values of critical temperature next to 17 K are expected for Nb_3Sn wires due to the thermal contraction of the Cu against Nb filaments, when they are cooled from the HT temperatures and measured in cryogenic temperatures.

Fig. 2 shows the curves of critical current densities J_c as a function of the applied magnetic field $\mu_0 H$ for samples after heat treatment, with the applied magnetic field perpendicular to the axis of the wires. Sample 7 is the worst result, showed in all graphics as parameter for comparison between different samples and HT. Fig. 2 also compares the samples treated with just one

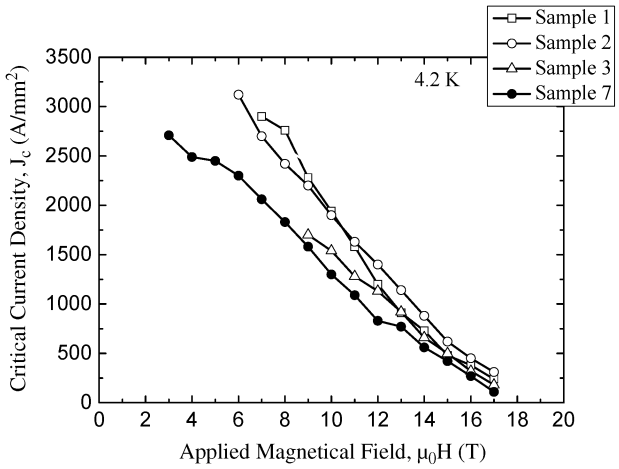

Fig. 2. Critical current densities versus applied magnetic field for samples 1, 2, and 3. Sample 7 is parameter for comparison.

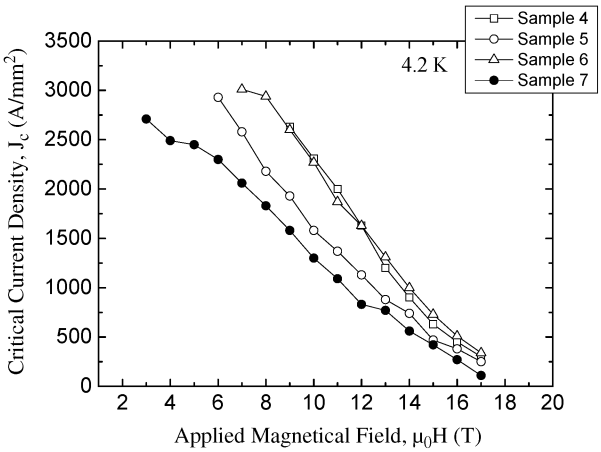

Fig. 3. Critical current densities versus applied magnetic field.

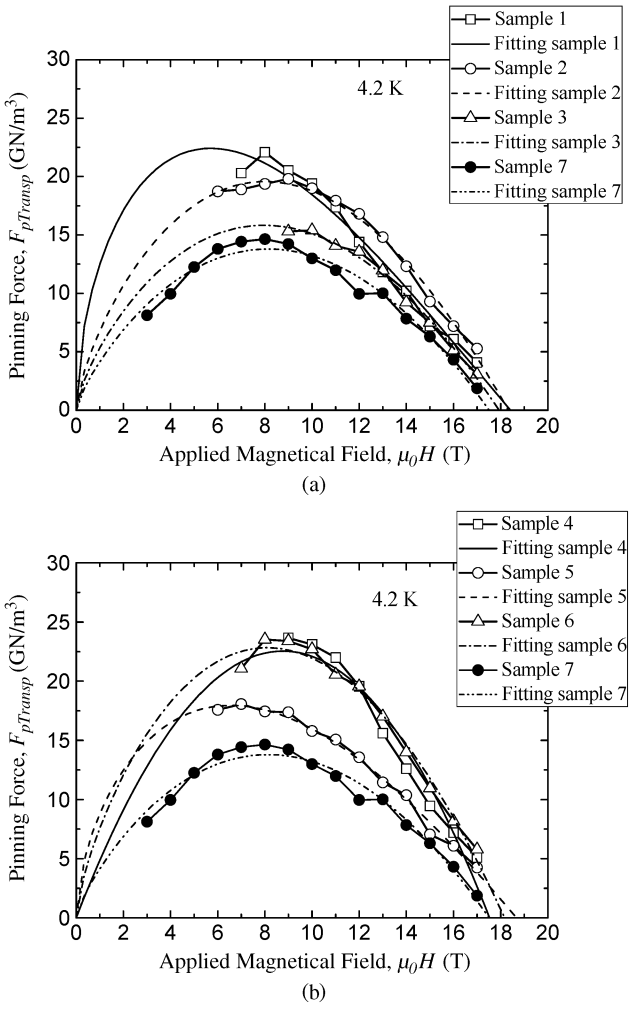

Fig. 4. (a) $J_{cTransp}$ vs. $\mu_0 H$ and (b) $F_{pTransp}$ vs. $\mu_0 H$. The fitting lines were obtained using Eq. (1) for each curves, with results listed in Table III.

step of HT at 575°C/200 h (sample 1), 650°C/200 h (sample 2), and 700°C/100 h (sample 3). In high applied magnetic field, between 11 and 17 T, sample 2 showed the higher values of critical current densities, while sample 1 showed better results at applied magnetic fields under 10 T. Sample 3 showed the worst results, with lower values of critical current densities in all measured fields. It means that high temperatures of annealing are not efficient for nanostructured superconducting wires, possibly due to the excessive grain growth and, consequently, lower efficiency of pinning of the magnetic flux lines.

Fig. 3 compares the samples treated with initial steps of HT at 220°C/100 h, 480°C/50 h, and 575°C/50 h, and final treatment at 650°C/50 h. It can be observed that there are no great differences between samples annealed with different initial step of HT. The comparison of samples heat treated with more than one step of intermediate HT, for example sample 7 $(220°\mathrm{C}/100\ \mathrm{h} + 480°\mathrm{C}/50\ \mathrm{h} + 650°\mathrm{C}/100\ \mathrm{h})$, leads to the conclusion that the intermediate HT is important for the superconducting performance of these nanostructured wires. It is probably due to the Cu-Sn diffusion process, because these superconducting wires were prepared using the solid-liquid approach. The HT at 480°C consumes much energy and Sn of the system due to the formation of the Cu-Sn δ phase, which is a very stable phase [10]. This behavior can be also observed for sample 5, treated at 480°C. The best values of the critical current densities were found for samples 4 and 6 in applied magnetic field below 11 T. On the other hand, the lower values of critical current densities were obtained for sample 7, in all analyzed applied magnetic fields.

Fig. 4 shows the curves of pinning force F_p as a function of the applied magnetic field $\mu_0 H$ for samples after HT and their respective fitting curves. Table III shows the results from the mathematical fitting of the curves presented in Fig. 4. These fittings were calculated using the expression:

$$\mathrm{F_p} = \mathrm{K}\left[x\mathrm{b}^{\frac{1}{2}}(1-\mathrm{b})^2 + (1-x)\mathrm{b}(1-\mathrm{b})\right] \qquad (1)$$

where K is a constant, $b = B/B_{c2}$ is the reduced magnetic field, and x is the contribution of the pinning mechanism related to the shearing of the magnetic flux lines at the grain boundaries. In this expression, the first term, $b^{1/2}(1-b)^2$, corresponds to this mechanism of flux pinning due to the grain boundaries, and the second term, $b(1-b)$, is the contribution of the pinning by the normal phases created with the introduction of the APCs into the superconducting phase.

The behavior of the curves in Fig. 4, and the values listed in Table III, show that the samples mixed pinning behaviors due to

TABLE III
TABLE FROM MATHEMATICAL FITTING OF $F_{PTransp}$ VS. M_0H (TRANSPORT PROPERTIES)

Sample	K (GN/m^3)	x	B_{C2} (T)	$B(F_{pmax})$ (T)	F_{pmax} (GN/m^3)	$b(F_{pmax})$
1	93.02	0.53	18.42	5.80	22.50	0.31
2	81.97	0.20	18.32	8.08	19.51	0.44
3	6.09	0.18	17.93	7.89	15.78	0.44
4	114.09	0.50	18.40	5.95	27.28	0.32
5	75.82	0.42	18.67	6.47	17.93	0.35
6	95.24	0.17	18.17	8.03	22.73	0.44
7	56.92	0.12	17.51	7.99	13.78	0.45

shearing of the flux line lattice at the grain boundaries and due to the pinning by the normal phases. These results suggest that the HT with just one step of treatment and those with intermediate step of HT at 480°C did not show satisfactory results.

These results are related to the formation of the superconducting phases and the form how the magnetic flux lines are pinned, in the presence of an applied magnetic field. The low values of J_c are mainly due to the excessive growth of the superconducting grains and the consequent decreased of grain boundary densities acting as pinning centers.

The values of x in Table III and the behavior of the curves in Fig. 4 lead to the conclusion that the high values of J_c for samples 4 and 6 have distinct explanations. Sample 4 has large and homogeneous superconducting phases, but without excessive growth of the Nb_3Sn grains. In this case, the flux pinning is more effective due to the pinning by shearing of flux lines at the grain boundaries acting simultaneously with the pinning by the APCs. Sample 6 has an excessive growth of the Nb_3Sn grains, but the introduction of the APCs acted effectively on the flux pinning. These APCs improved the critical current densities, via proximity effect [11].

The HT at 575°C/200 h (sample 1), considered of poor kinetics for conventional Nb_3Sn superconductors, already formed superconducting phases capable of transporting high current densities and showed high values of upper critical magnetic field. This is a direct consequence of the low dimensions of the nanometric-scale APCs and Nb filaments. The HT at 575°C showed values of critical current densities and pinning mechanism similar to the other samples treated at higher temperatures. This shows that this new nanostructured superconducting wires do not require high temperatures to form homogeneous Nb_3Sn superconducting phases due to the nanometric dimensions and distribution of the Nb filaments, and the introduction of the APCs.

Sample 7 shows the worst values of $J_{cTransp}$. The treatment at 480°C prejudiced the superconducting phase, probably due to the formation of the Cu-Sn δ phase, which retained Sn and, consequently, lead to a lower content of Sn in the Nb_3Sn phase [12]. On the other hand, samples 1, 2, 4, and 6 showed similar values of critical current densities, but higher than those for the other samples. This is a indication of the good quality of the superconducting phase formed in these samples.

IV. CONCLUSION

This work showed that heat treatments used for conventional Nb_3Sn wires cannot be applied for nanostructured superconducting wires and new heat treatment profiles must be determined. Heat treatment optimization for these nanostructured superconductors shows that intermediate steps are required.

Due to the nanometric dimensions of the APCs and the Nb filaments, heat treatments at 575°C were already enough to promote the formation of superconducting phases capable of transporting high current densities. Low annealing temperatures and short annealing times already formed the superconducting phases. On the other hand, the Nb_3Sn average grain sizes were kept small and the pinning mechanism was determined as mainly due to the grain boundaries mixed to the normal phases obtained with the introduction of the APCs.

ACKNOWLEDGMENT

The authors thank the Institute of Physics, USP, Brazil, for the use of the 17T magnet during the Ic measurements; LME-LNLS, Campinas, Brazil, for the use of FEG-SEM. The electron microscopy work was performed at the Laboratório Nacional de Luz Síncrotron (LNLS), Campinas, SP, Brazil.

REFERENCES

[1] Z. Chaowu, A. Sulpice, Z. Lian, J. L. Soubeyroux, C. Verwaerde, and G. K. Hoang, *IEEE Trans. Appl. Superc.*, vol. 17, pp. 7–12, 2007.
[2] P. Wanderer, " Nb_3Sn magnet development for LHC luminosity upgrade," in *CERN European Organization for Nuclear Research, WAMSDO Workshop Accelerator Magnet Superconductors, Design and Optimization CERN*, Geneva, Switzerland, 2008, pp. 108–113.
[3] C. A. Rodrigues and D. Rodrigues, Jr., *IEEE Trans. Appl. Superc.*, vol. 17, pp. 2627–2630, 2007.
[4] C. A. Rodrigues, J. P. B. Machado, and D. Rodrigues, Jr., *IEEE Trans. Appl. Superc.*, vol. 13, pp. 3426–3429, 2003.
[5] L. B. S. Da Silva, C. A. Rodrigues, C. Bormio-Nunes, N. F. Oliveira, Jr., and D. Rodrigues, Jr., *Journal of Physics: Conference Series*, vol. 167, p. 012012, 2009.
[6] M. Müller, H. Schulz, and H. Kirchmayr, *Physica C*, vol. 419, pp. 115–120, 2005.
[7] H. Müller and T. Schneider, *Physica C*, vol. 401, pp. 325–329, 2004.
[8] *British Standard, Superconductivity—Part 10: Critical Temperature Measurement—Critical Temperature of Composite Superconductors by a Resistance Method*, BS EN 61788-10, 2006.
[9] *British Standard, Superconductivity—Part 2: Critical Current Measurement—DC Critical Current of* Nb_3Sn *Composite Superconductors*, BS EN 61788-2, 2007.
[10] M. T. Naus, P. J. Lee, and D. C. , *IEEE Trans. Appl. Superc.*, vol. 11, pp. 2569–2572, 2001.
[11] D. Rodrigues, Jr., C. A. Rodrigues, E. B. Silveira, and E. G. M. Romão, *IEEE Trans. Appl. Superc.*, vol. 15, pp. 3389–3392, 2005.
[12] M. Suenaga, , B. B. Schwartz and S. Foner, Eds., *Superconductor Material Science-Metallurgy, Fabrication and Applications*. New York: Plenum Press, 1981, vol. 4, p. 201.